

Hypertension

JOURNAL OF THE AMERICAN HEART ASSOCIATION



*Learn and Live*SM

Pioglitazone Improves Aortic Wall Elasticity in a Rat Model of Elastocalcinotic Arteriosclerosis

Virginie Gaillard, Daniel Casellas, Carole Seguin-Devaux, Hervé Schohn, Michel Dauça, Jeffrey Atkinson and Isabelle Lartaud

Hypertension 2005;46;372-379; originally published online Jun 20, 2005;

DOI: 10.1161/01.HYP.0000171472.24422.33

Hypertension is published by the American Heart Association, 7272 Greenville Avenue, Dallas, TX 75214

Copyright © 2005 American Heart Association. All rights reserved. Print ISSN: 0194-911X. Online ISSN: 1524-4563

The online version of this article, along with updated information and services, is located on the World Wide Web at:

<http://hyper.ahajournals.org/cgi/content/full/46/2/372>

Subscriptions: Information about subscribing to Hypertension is online at
<http://hyper.ahajournals.org/subscriptions/>

Permissions: Permissions & Rights Desk, Lippincott Williams & Wilkins, a division of Wolters Kluwer Health, 351 West Camden Street, Baltimore, MD 21202-2436. Phone: 410-528-4050. Fax: 410-528-8550. E-mail:
journalpermissions@lww.com

Reprints: Information about reprints can be found online at
<http://www.lww.com/reprints>

Pioglitazone Improves Aortic Wall Elasticity in a Rat Model of Elastocalcinotic Arteriosclerosis

Virginie Gaillard, Daniel Casellas, Carole Seguin-Devaux, Hervé Schohn, Michel Dauça, Jeffrey Atkinson, Isabelle Lartaud

Abstract—Specific treatment of age-related aortic wall arteriosclerosis and stiffening is lacking. Because ligands for peroxisome proliferator-activated receptor γ have beneficial effects on the arterial wall in atherosclerosis, via an antiinflammatory mechanism, we investigated whether long-term pioglitazone (Pio) treatment protects against another form of vascular wall disease, arteriosclerosis. We evaluated, in a rat model of elastocalcinotic arteriosclerosis (hypervitaminosis D and nicotine [VDN]), whether Pio (3 mg \cdot kg⁻¹ per day for 1.5 month PO) attenuated arteriosclerosis and its consequences: aortic wall rigidity, increased aortic pulse pressure, and left ventricular hypertrophy. In VDN rats, medial calcification was associated with monocyte/macrophage infiltration and induction of tumor necrosis factor α and interleukin 1 β . Pio increased nuclear peroxisome proliferator-activated receptor γ immunostaining in the aortic wall, decreased tumor necrosis factor α ($P < 0.05$ versus VDN Pio⁻), tended to decrease interleukin 1 β mRNA expression ($P = 0.08$ versus VDN Pio⁻), blunted aortic wall calcification (271 ± 69 , $P < 0.05$ versus VDN Pio⁻ 562 ± 87 $\mu\text{mol} \cdot \text{g}^{-1}$ dry weight) and prevented fragmentation of elastic fibers (segments per 10 000 μm^2 : 8.4 ± 0.3 ; $P < 0.05$ versus VDN Pio⁻ 10.5 ± 0.6). Pio reduced aortic wall stiffness (elastic modulus/wall stress: 4.8 ± 0.6 ; $P < 0.05$ versus VDN Pio⁻ 10.0 ± 1.6), aortic pulse pressure (30 ± 2 mm Hg; $P < 0.05$ versus VDN Pio⁻ 39 ± 4) and left ventricular hypertrophy (1.58 ± 0.05 g \cdot kg⁻¹; $P < 0.05$ versus VDN Pio⁻ 1.76 ± 0.06). In conclusion, long-term Pio treatment attenuates aortic wall elastocalcinosis and, thus, lowers aortic wall stiffness, aortic pulse pressure, and left ventricular hypertrophy. (*Hypertension*. 2005;46:372-379.)

Key Words: extracellular matrix ■ peroxisome proliferator-activated receptor ■ arteriosclerosis ■ calcium ■ pulse pressure

An age-related increase in aortic wall stiffness is an independent risk factor for cardiovascular morbidity and mortality.¹⁻³ There is no specific treatment, thus the research for drug targets is of great importance. Aortic wall stiffening arises principally from extracellular matrix remodeling of the media. Calcification and fragmentation of the elastic fiber network,^{4,5} and nonenzymatic cross-linking (glycation)^{6,7} of collagen fibers, are the most important determinants.

Several of these molecular mechanisms (calcification, glycation) have an inflammatory element. Thus, we investigated a new antiinflammatory pharmacological target, the peroxisome proliferator-activated receptor (PPAR)- γ , on the basis that thiazolidinediones (TZDs) specific PPAR- γ ligands have beneficial protective effects on the arterial wall in atherosclerosis^{8,9} and arteriosclerosis,¹⁰ via antiinflammatory mechanisms.

The beneficial antiproliferative and antifibrotic effects of pioglitazone (Pio) were demonstrated using a rat model of inflammation-induced wall fibrosis (long-term inhibi-

tion of endothelial NO synthesis).¹⁰ In the present study, we focused on another determinant of extracellular matrix remodeling: medial elastocalcinosis. We used an animal model of calcification and degradation of elastic fibers, the rat treated with vitamin D₃ and nicotine (VDN).¹¹⁻¹³ To our knowledge, this is the only model showing extensive aortic medial calcification, in the absence of fibrosis or any change in wall stress. In VDN rats, extracellular calcium-binding proteins and ectopic apatite deposition develop on medial elastic fibers, followed by fragmentation of the latter (elastocalcinosis).^{11,12} This causes wall stiffening, then elevation of pulse arterial pressure (with no change in mean arterial pressure) and compensatory left ventricular hypertrophy.^{12,13}

Our working hypotheses were that (1) VDN-induced calcification and elastic fiber fragmentation represent, at least partially, an inflammatory response of the aortic wall; and (2) long-term treatment of VDN rats with Pio¹⁰ (Pio), by counteracting the inflammatory process,⁸⁻¹⁰ reduces calcification and elastic fiber fragmentation, therefore leading to a de-

Received October 26, 2004; first decision November 16, 2004; revision accepted May 11, 2005.

From the Unité Mixte UHP-INSERM U684, Pharmacology Laboratory Faculté de Pharmacie (V.G., J.A., I.L.), and Faculté de Médecine (C.S.-D.), Université Henri Poincaré Nancy-1, Nancy; Groupe Rein et Hypertension (EA3127) (D.C.), Institut Universitaire de Recherche Clinique, Montpellier; Peroxisome Proliferators (EA 3446) (H.S., M.D.), Faculté des Sciences et Techniques, Université Henri Poincaré Nancy-1, Nancy, France.

Correspondence to Jeffrey Atkinson, Pharmacology Laboratory, UHP-INSERM U684, Faculté de Pharmacie de l'Université Henri Poincaré, Nancy I, 5 rue Albert Lebrun, 54 000 Nancy, France. E-mail Jeffrey.Atkinson@pharma.uhp-nancy.fr

© 2005 American Heart Association, Inc.

Hypertension is available at <http://www.hypertensionaha.org>

DOI: 10.1161/01.HYP.0000171472.24422.33

crease in wall elastic modulus and the consequences of increased aortic wall rigidity, namely, increased pulse pressure and left ventricular hypertrophy. In a separate experiment, we checked whether the beneficial effect of Pio was attributable to a short-term, functional, or long-term structural effect on the aortic wall.

Methods

Animals and Drug Treatment

Seven-week-old male Wistar rats (Ico: Wi, IOPS AF/Han, Charles River Laboratories, L'Arbresle, France) were kept under standard conditions for 1 week before VDN treatment.

For the long-term experiment, VDN rats ($n=26$) were treated on day 0 (D_0) with vitamin D_3 ($300\,000\text{ IU}\cdot\text{kg}^{-1}\text{ IM}$) and nicotine ($2\times 25\text{ mg}\cdot\text{kg}^{-1}$, $5\text{ mL}\cdot\text{kg}^{-1}\text{ PO}$)¹¹⁻¹³; non-VDN rats ($n=22$) were treated with $0.15\text{ mol/L NaCl (IM)}$ and distilled water (PO). From D_1 to D_{44} , rats received Pio ($3\text{ mg}\cdot\text{kg}^{-1}$ per day, $6\text{ mL}\cdot\text{kg}^{-1}$; $n=17$ VDN Pio⁺ and 13 non-VDN Pio⁺ rats) or carboxymethylcellulose (0.5% , $6\text{ mL}\cdot\text{kg}^{-1}$; $n=9$ VDN Pio⁻ and 9 non-VDN Pio⁻ rats) PO at 12:00 PM. We used the same treatment schedule as Ishibashi et al, who reported that $3\text{ mg}\cdot\text{kg}^{-1}$ per day of Pio had beneficial antiproliferative and antifibrotic effects on the coronary artery wall in a rat model of inflammation-induced wall fibrosis.¹⁰ Hemodynamic parameters were measured on D_{45} (24-hour drug washout) under sodium pentobarbital anesthesia ($60\text{ mg}\cdot\text{kg}^{-1}\text{ IP}$). Experiments followed the guidelines of the French Ministry of Agriculture, Paris (permit numbers IL: 54-5 and JA: 03575).

In a separate experiment, 12 VDN and 10 non-VDN rats received on D_{45} , 1 gavage of Pio ($3\text{ mg}\cdot\text{kg}^{-1}$) or carboxymethylcellulose at 12:00 PM. Hemodynamic parameters were measured 2 hours later (time of the peak in the plasma concentration of Pio, high-performance liquid chromatography/UV, results not shown).

Aortic Blood Pressure and Pulse Wave Velocity

On D_{45} , polyethylene cannula, connected to low-volume pressure transducers, were introduced into the descending thoracic and abdominal aorta for measurement of baseline central and peripheral blood pressures.^{6,12-15} An algorithm detected systolic and diastolic

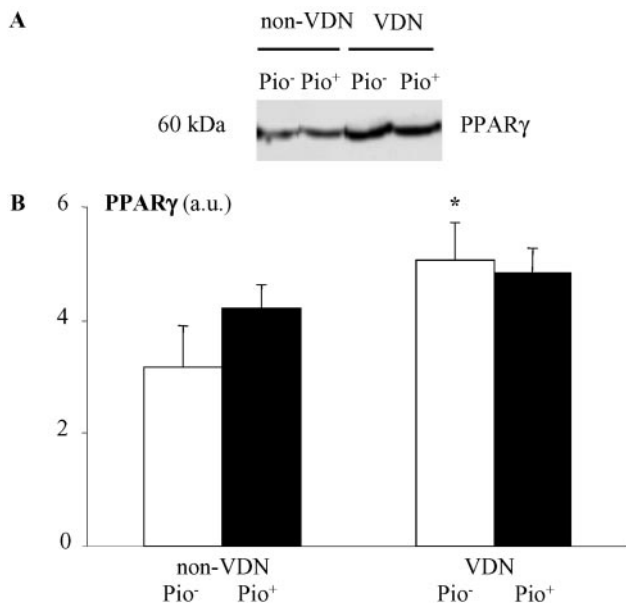


Figure 1. Western blot analysis of PPAR- γ protein in VDN and non-VDN rats, treated or not with Pio for 44 days. A, Representative examples of the bands obtained. B, Densitometric quantification. $*P<0.05$ vs non-VDN. $P_{\text{VDN}}=0.050$, $P_{\text{Pio}}=0.512$, $P_{\text{VDN}\times\text{Pio}}=0.299$.

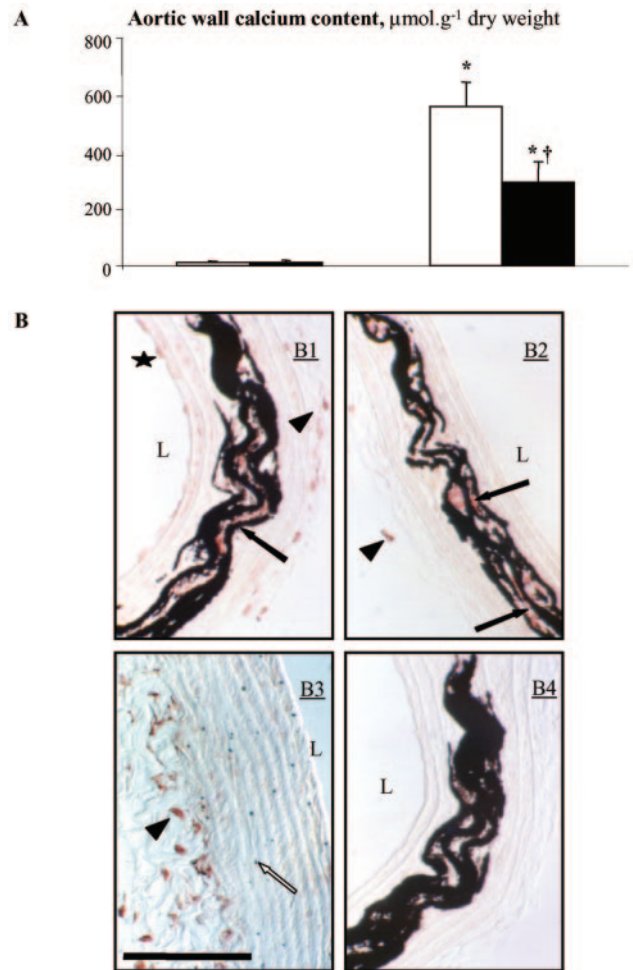


Figure 2. A, Total calcium content of the thoracic aortic wall in VDN and non-VDN rats, treated or not with Pio for 44 days. $*P<0.05$ vs non-VDN rats, $\dagger P<0.05$ vs Pio⁻. $P_{\text{VDN}}<10^{-4}$, $P_{\text{Pio}}=0.036$, $P_{\text{VDN}\times\text{Pio}}=0.047$. B, Light microscopic views of the aortic wall in a VDN rat. B1 to B3, Successive sections of the same aorta. Calcium was revealed by the Von Kossa stain (black deposits); monocyte/macrophages were immunostained with a monoclonal mouse anti-rat ED-1 (red deposits). B1 and B2, Intense calcium deposition along the elastic lamellae. Monocyte/macrophages are present between the calcified lamellae (black arrows), within the adventitia (black arrowheads), and at the surface of the endothelium (black star). B3, Sparse calcium deposits (white arrow) and monocyte/macrophage infiltration within the adventitia (black arrowhead). The anti-ED-1-antibody was omitted in the adjacent aortic section, and B4 depicts the area shown in B1. Bar indicates 100 micrometers (applies to all panels); L, lumen.

pressures, calculated mean pressure (waveform area), pulse pressure (systolic-diastolic), heart rate and thoraco-abdominal pulse wave transit time.^{6,12-15} Pulse wave velocity (PWV) was calculated as the distance between the 2 cannula tips (measured in situ following euthanasia) divided by the pulse wave transit time.

The impact of sodium pentobarbital on hemodynamic values must be considered because a decrease in sympathetic nervous system activity (1) lowers aortic smooth muscle cell tone, which could modify elasticity per se (however, we previously showed that a change in local smooth muscle cell tone is not an important determinant of aortic wall elasticity¹⁴); (2) may lower blood pressure and thus wall stress (however, in the present study, mean aortic blood pressure was similar in non-VDN and VDN rats [as we reported for awake animals¹³]); and (3) would lower heart rate and thus change

the harmonic composition of the pulse pressure signal. This would alter PWV measured, as it did here (by the foot-to-foot method). However, changes in heart rate were relatively minor (see Results).

Plasma Glucose Concentration, Left Ventricular Weight, Thoracic Aorta Geometry and Mechanics, and Wall Elastic Network

One milliliter of arterial blood was collected for determination of plasma glucose (glucose oxidase method). After euthanasia (sodium pentobarbital overdose), the left ventricle, including septum, was dissected free and weighed; left ventricular hypertrophy was estimated as left ventricle/body weight. The apex of the ventricle (150 mg) was dehydrated at 110°C to determine the percentage of dry weight.

The first centimeter of the descending thoracic aorta (location in study by Niederhoffer et al¹²) was removed, fixed in formaldehyde (10% in phosphate buffered saline), and embedded in paraffin for histomorphometric analyses and evaluation of monocyte/macrophage infiltration (see above). All tests were performed by 2 independent, blinded observers. The internal diameter (D_i) and medial thickness (h) were measured on 20- μ m thick sections stained with hematoxylin-eosin (Saisam algorithm; Microvision Instruments, Evry, France).

Elastic modulus ($EM = PWV^2 \cdot D_i \cdot \rho / h$; Moens-Korteweg) and wall stress ($WS = \text{central aortic mean blood pressure} \cdot D_i / 2 h$; Lamé) were calculated with $\rho = \text{blood density}$, 1.05 g \cdot cm⁻³. EM/WS was used as an isobaric index of intrinsic aortic wall stiffness.^{6,15}

Fragmentation of the medial elastic fiber network (excluding the external and internal laminae) was evaluated on 10- μ m thick sections stained with Weigert solution by measuring the increase in the number¹⁵ and the decrease in the length of elastic lamellae.

Monocyte/Macrophage Infiltration in the Aortic Wall, Interferon γ , Tumor Necrosis Factor α , and Interleukin 1 β mRNA Expression

Aortic calcium was visualized as black deposits on deparaffinized/rehydrated sections using the Von Kossa stain.^{11,16} Sections were then antigen-retrieved in citrate buffer (pH 6, 40 minutes, 97°C then 20 minutes, room temperature). Monocyte/macrophages were immunostained by overnight exposure (4°C) to a monoclonal mouse anti-rat ED-1 antibody (dilution 1:500; mca341r, Serotec, UK). The antibody was revealed as red deposits using an indirect streptavidin-biotin method with H₂O 2/3-amino-9-ethylcarbazole as chromogen (DAKO Chemmate Detection Kit; peroxidase).

Total mRNA was extracted from the second centimeter¹² of the descending thoracic aorta (6 to 9 rats per group) using Tri-Reagent (Euromedex, Souffelweyersheim, France) and RNEASY Mini Kit (Qiagen, Courtaboeuf, France). Total mRNA concentration was measured, its integrity was confirmed, and reverse transcription-polymerase chain reaction (PCR) and PCR were performed as previously described^{17,18} (using the housekeeping gene L27: amplimers 5'-TCCTGGCTGGACGCTACTC-3', sense; and 5'-CCACAGAGTACCTTGTTGGGC-3', antisense; annealing temperature 62°C, PCR product 225 bp). The PCR products (separated on a 2% agarose gel containing 0.5 μ g \cdot mL⁻¹ ethidium bromide) were quantified as density ratio (PCR product of interest/L27) by densitometry (Bio-Rad Gel Doc 1000; Bio-Rad Laboratories).

Thoracic Aorta Wall Composition

The third centimeter¹² of the descending thoracic aorta was hydrolyzed in hydrochloric acid (6 mol/L, 24 hour, 105°C) and protein (molecular weight of an amino acid, 92; dinitrofluorobenzene reaction)¹⁹ and collagen (hydroxyproline content, 7.46 \times ; chloramine T and paradimethylaminobenzaldehyde reaction)²⁰ contents determined.

The fourth centimeter¹² of the descending thoracic aorta was dehydrated at 110°C to determine the percentage of dry weight and total wall calcium content (atomic absorption spectrophotometry following mineralization and nitric acid digestion).¹¹

Quantification and Localization of PPAR- γ in the Aortic Wall

The second centimeter¹² of the descending thoracic aorta was used for Western blot analysis. Each aorta was analyzed in triplicate as previously described,²¹ using a polyclonal rabbit PPAR- γ anti-serum²² (dilution 1:1500) then luminol (Mouse/Rabbit chemoluminescence detection kit; Roche) and quantified by densitometry (GelDoc; Bio-Rad).

The ascending aorta (embedded in freezing medium) was used for immunostaining (3- μ m thick sections; polyclonal rabbit PPAR- γ anti-serum²² [dilution 1:500]; fluorescein-conjugated goat anti-rabbit IgG [1:50]; UV microscopy).²² The analysis was performed on 3 to 4 rats per group, 3 aortic sections per rat, focusing on 30 to 40 medial smooth muscle cells per section, to evaluate the percentage of smooth muscle cells showing nuclear PPAR- γ staining.

Statistics

Parametric values (means \pm SEM) were analyzed by a 2-way ANOVA (P_{VDN} , P_{Pio} , $P_{VDN \times Pio}$) plus the Bonferroni post hoc test and nonparametric values (immunostaining) by the Mann-Whitney U

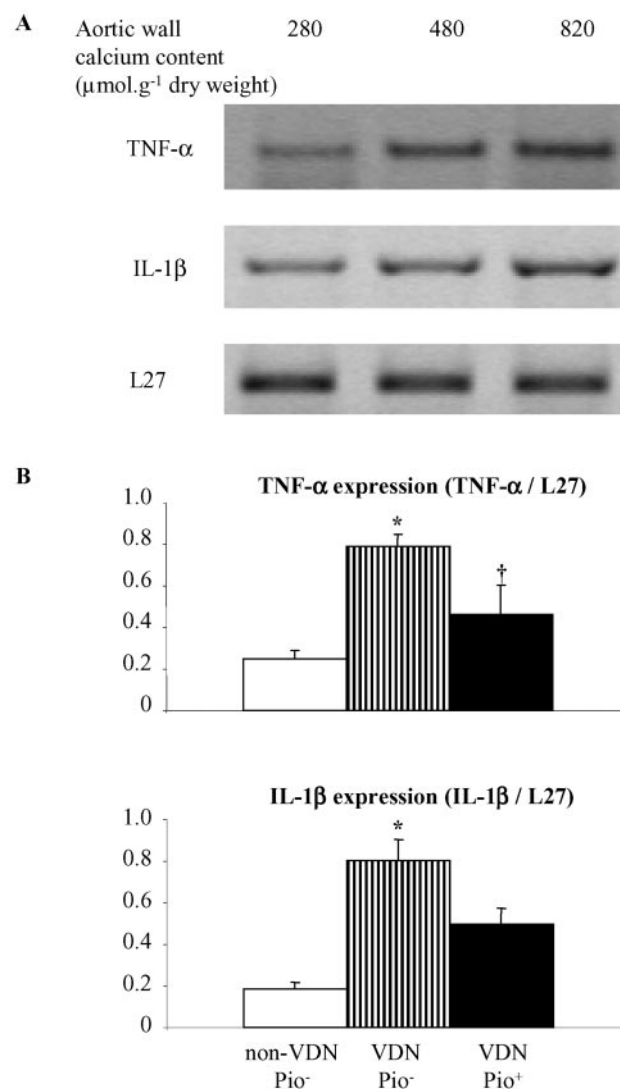


Figure 3. TNF- α and IL-1 β mRNA expression in the aortic wall of VDN and non-VDN rats treated or not with Pio for 44 days. A, Representative examples of the bands obtained. B, Densitometric quantification. P value for one-way ANOVA: TNF- α =0.0003, IL-1 β =0.0003. * P <0.05 vs non-VDN Pio^- , † P <0.05 vs Pio^- .

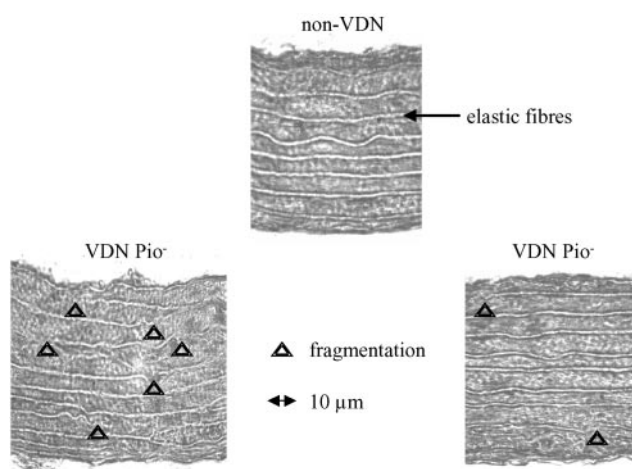


Figure 4. Elastic network (Weigert) of the thoracic aortic media in representative rats from the non-VDN and VDN groups, treated or not with Pio. L indicates lumen; A, adventitia.

test. Linear regressions were performed using standard ANOVA techniques and results expressed as slopes and intercepts.

Drugs

Vitamin D₃ (Duphafrol D₃) was purchased from Duphar B.V. (Weesp, The Netherlands), sodium pentobarbital from Sanofi Santé Nutrition Animale (Libourne, France), and other chemicals from

Sigma Chemical Co (St Louis, Mo). Pio was a gift of Takeda Chemicals Industries Ltd (Osaka, Japan).

Results

PPAR- γ , Monocyte/Macrophage Infiltration, Cytokine Expression, Elastic Network, Composition of the Aortic Wall, and Thoracic Aorta Geometry

VDN treatment increased PPAR- γ protein content (1.6 \times), but long-term treatment with Pio had no effect (Western blot, Figure 1). Medial smooth muscle cells presented positive cytoplasmic immunostaining for PPAR- γ , with no difference between non-VDN and VDN. Pio⁺ increased nuclear PPAR- γ staining to 95 \pm 2% (non-VDN Pio⁺+VDN Pio⁺ rats, P <0.05 versus 65 \pm 10% in non-VDN Pio⁻+VDN Pio⁻ rats).

The calcium content of the aortic wall increased 43 \times in VDN rats (Figure 2); Pio⁺ partially prevented calcification (VDN Pio⁺: 21 \times versus non-VDN rats). In VDN rats, the media exhibited heavy calcium deposits along the elastic lamellae and monocyte/macrophage infiltration between calcified lamellae (Figure 2). In VDN Pio⁺, the occurrence of calcified lesions along the aortic segment was lower, but, when present, lesions were similar in nature to those observed in VDN Pio⁻ and showed monocyte/macrophage infiltration.

TABLE 1. Thoracic Aorta Geometry, Elastic Network, and Composition of the Aortic Wall of VDN and Non-VDN Rats Treated or Not With Pio for 44 Days

Groups	Non-VDN	VDN	ANOVA		
Aortic geometry					
D _i , mm					
Pio ⁻	1.85 \pm 0.06	2.28 \pm 0.10*	P_{VDN} =0.001	P_{Pio} =0.046	$P_{VDN \times Pio}$ =0.013
Pio ⁺	1.89 \pm 0.04	1.96 \pm 0.06†			
Medial thickness, μ m					
Pio ⁻	72 \pm 3	78 \pm 2	P_{VDN} =0.144	P_{Pio} =0.392	$P_{VDN \times Pio}$ =0.368
Pio ⁺	72 \pm 2	74 \pm 2			
Elastic fiber fragmentation					
No. of medial elastic segments per 10 000 μ m ²					
Pio ⁻	8.0 \pm 0.3	10.5 \pm 0.6*	P_{VDN} <10 ⁻⁴	P_{Pio} =0.002	$P_{VDN \times Pio}$ =0.043
Pio ⁺	7.6 \pm 0.3	8.4 \pm 0.3†			
Ratio of the length of elastic fibers to the length of the medial area section					
Pio ⁻	0.95 \pm 0.03	0.61 \pm 0.04*	P_{VDN} <10 ⁻⁴	P_{Pio} <10 ⁻⁴	$P_{VDN \times Pio}$ =0.001
Pio ⁺	1.00 \pm 0.02	0.88 \pm 0.03*†			
Aortic wall composition					
Dry weight/wet weight, %					
Pio ⁻	42 \pm 1	46 \pm 2	P_{VDN} =0.312	P_{Pio} =0.624	$P_{VDN \times Pio}$ =0.186
Pio ⁺	44 \pm 1	43 \pm 2			
Total protein content, mg \cdot g ⁻¹ wet weight					
Pio ⁻	322 \pm 13	268 \pm 16*	P_{VDN} =0.025	P_{Pio} =0.431	$P_{VDN \times Pio}$ =0.167
Pio ⁺	313 \pm 11	299 \pm 13			
Collagen content, mg \cdot g ⁻¹ wet weight					
Pio ⁻	135 \pm 9	123 \pm 8	P_{VDN} =0.298	P_{Pio} =0.944	$P_{VDN \times Pio}$ =0.970
Pio ⁺	134 \pm 4	128 \pm 5			

* P <0.05 vs non-VDN rats, † P <0.05 vs Pio⁻.

TABLE 2. Central Aortic Blood Pressure, Wall Stress, and Pulse Wave Velocity in Anesthetized VDN and Non-VDN Rats Treated or Not With Pio for Forty-Four Days

Groups	Non-VDN	VDN	ANOVA		
Central aortic blood pressure, mm Hg					
Mean					
Pio ⁻	109±3	107±4	$P_{VDN}=0.407$	$P_{Pio}=0.598$	$P_{VDN \times Pio}=0.111$
Pio ⁺	106±4	114±2			
Systolic					
Pio ⁻	122±3	127±5	$P_{VDN}=0.009$	$P_{Pio}=0.724$	$P_{VDN \times Pio}=0.304$
Pio ⁺	117±3	130±2*			
Diastolic					
Pio ⁻	97±3	88±4	$P_{VDN}=0.519$	$P_{Pio}=0.303$	$P_{VDN \times Pio}=0.056$
Pio ⁺	94±4	98±2†			
Wall stress, 10 ⁶ dynes · cm ⁻²					
Pio ⁻	1.87±0.11	2.01±0.04	$P_{VDN}=0.120$	$P_{Pio}=0.852$	$P_{VDN \times Pio}=0.835$
Pio ⁺	1.86±0.10	2.05±0.09			
PWV, cm · s ⁻¹					
Pio ⁻	494±26	752±63*	$P_{VDN} < 10^{-4}$	$P_{Pio}=0.015$	$P_{VDN \times Pio}=0.043$
Pio ⁺	477±23	571±52†			

* $P < 0.05$ vs non-VDN rats, † $P < 0.05$ vs Pio⁻.

Interferon γ mRNA content did not change in VDN rats (results not shown), but tumor necrosis factor (TNF)- α and interleukin (IL)-1 β mRNA expression increased in parallel with the degree of calcification (Figure 3). There was a significant positive relationship between IL-1 β expression and calcium content of the aortic wall in VDN Pio⁻ rats (slope ($\times 10^{-4}$)=9.8±1.7 $\mu\text{mol}^{-1} \cdot \text{g}$; $r=0.9035$; $P < 0.05$; intercept=0.25±0.11; $n=9$) but not between TNF- α and calcium content. Pio⁺ decreased TNF- α ($P < 0.05$ versus VDN Pio⁻) and tended to decrease IL-1 β ($P=0.08$) expression by 38% and 25%, respectively. In VDN Pio⁺, the correlation between IL-1 β and calcium content of the wall was not statistically significant.

The medial elastic network showed severe fragmentation and disorganization in VDN rats (Figure 4), with an increase in the number (+31%) and a decrease in the length (-36%) of lamellae (Table 1). Pio⁺ blunted elastic network fragmentation in VDN rats.

The dry weight and collagen content of the aortic wall were similar in all groups (Table 1). Protein content decreased in VDN rats (-17%); Pio⁺ had no effect.

Internal diameter increased by 22% ($P < 0.05$) in VDN rats, with no change in medial thickness (Table 1). Chronic Pio treatment prevented dilatation in VDN rats but had no effect on medial thickness.

Aortic Blood Pressure and Wall Mechanics

PWV ($\times 1.5$, Table 2) and EM/WS ($\times 2.8$, Figure 5) increased in VDN rats, with no change in wall stress (Table 2). Pio⁺ decreased PWV and EM/WS in VDN rats only ($P_{VDN \times Pio} < 0.05$) to values that were not significantly different from those of non-VDN Pio⁻ rats (PWV, $P=0.150$; EM/WS, $P=0.189$).

There was a significant positive relationship between EM/WS and calcium content of the aortic wall in VDN

rats (slope=0.0074±0.0015 $\mu\text{mol}^{-1} \cdot \text{g}$; $r=0.719$; $P < 0.05$; intercept=3.44±0.77; $n=26$) but not in non-VDN rats. The linear regression slope for VDN Pio⁺ rats (0.0061±0.0017 $\mu\text{mol}^{-1} \cdot \text{g}$; $r=0.697$; $P < 0.05$; intercept=3.65±0.73; $n=17$) was lower ($P=0.0018$) than that for VDN Pio⁻ rats (0.0093±0.0041 $\mu\text{mol}^{-1} \cdot \text{g}$; $r=0.678$; $P=0.05$; intercept=2.69±2.59; $n=9$).

Central aortic mean blood pressure was similar in all groups (Table 2); pulse pressure increased by 56% in VDN rats (Figure 4). Pio lowered aortic pulse pressure (Figure 4) to a value not significantly different from that of non-VDN Pio⁻ rats ($P=0.083$).

In the short-term experiment, VDN Pio⁻ rats showed calcification and stiffening (calcium content 46 \times , PWV 1.5 \times non-VDN) of the aortic wall; pulse pressure increased by 61% versus non-VDN, with no change in mean aortic blood pressure or heart rate. Acute Pio administration had no effect on aortic wall calcium content, PWV or pulse pressure; it slightly increased mean aortic pressure (+4%) and decreased heart rate (-10%) both in VDN and non-VDN rats ($P < 0.05$).

Body Weight, Plasma Glucose Concentration, and Cardiac Parameters

VDN rats lost weight between D₀ and D₆ (-18%, results not shown), then recovered normal growth. At D₄₅, body weight was 5% lower in VDN than in non-VDN rats (Table 3). Pio⁺ increased body weight in both VDN and non-VDN rats (+10%). Plasma glucose concentrations were similar in all groups (Table 3).

Heart rate, left ventricle weight, and the percentage of myocardium dry weight were similar in all groups (Table 3). Left ventricle/body weight increased by 16% in VDN rats (Figure 5); Pio lowered this ratio to a value not significantly different from that of non-VDN Pio⁻ rats ($P=0.150$).

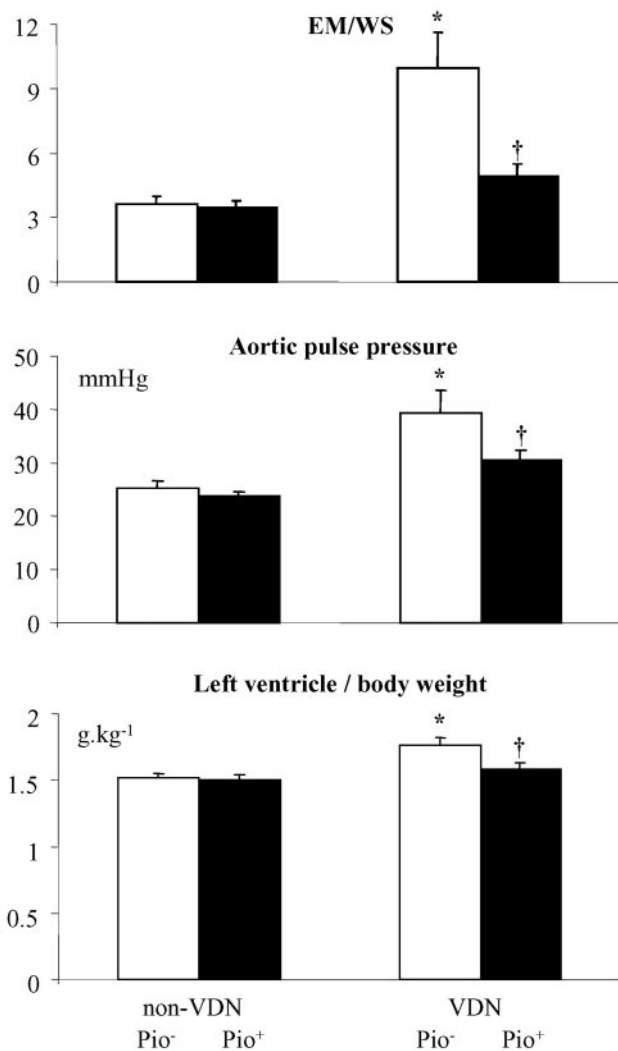


Figure 5. Elastic modulus to wall stress ratio of the thoracic aorta, aortic pulse pressure, and left ventricle/body weight in VDN and non-VDN rats treated or not with Pio for 44 days. * $P < 0.05$ vs non-VDN rats, † $P < 0.05$ vs Pio⁻. EM/WS: $P_{VDN} < 10^{-4}$, $P_{Pio} = 0.001$, $P_{VDN \times Pio} = 0.002$; Pulse pressure: $P_{VDN} < 10^{-4}$, $P_{Pio} = 0.030$, $P_{VDN \times Pio} = 0.123$; Left ventricle/body weight $P_{VDN} = 0.002$, $P_{Pio} = 0.042$, $P_{VDN \times Pio} = 0.111$.

Discussion

VDN treatment reveals an inflammatory response of the aortic wall (monocyte/macrophage infiltration and induction of proinflammatory cytokines) that accompanies calcification associated with medial elastic fiber fragmentation and wall stiffening. Treatment of VDN rats with Pio, which purportedly acts as an antiinflammatory agent in the arterial wall,^{8–10,23} blunts elastocalcinosis and its structural and hemodynamic consequences. Whether this is attributable to an antiinflammatory effect is discussed below.

The beneficial effect of Pio on vascular structure and hemodynamics was attributable not to a short-term but to a long-term effect; with short-term administration, Pio had no effect on aortic wall calcium content, PWV, or pulse pressure.

The anticalcinotic effect of Pio in VDN is more likely to be caused by activation of PPAR- γ rather than to a change in PPAR- γ expression. Pio treatment did not induce any change

in the PPAR- γ protein content in VDN, and the decrease in aortic wall calcium content did not correlate with changes in PPAR- γ levels. VDN treatment itself causes a significant increase in PPAR- γ (30% to 40%). Thus, although Pio tended to increase PPAR- γ in non-VDN rats, it does not produce any further significant increase in VDN rats. This does not exclude that nuclear activation of PPAR- γ by Pio may induce expression of target genes involved in the anticalcinotic effect. Another possibility is that PPAR- γ expression increases at an early stage of Pio treatment in VDN rats (and produces an anticalcinotic effect) and that later (D₄₅) the anticalcinotic effect remains, but the difference in PPAR- γ expression is masked.

An antiinflammatory action of Pio (witnessed by the decreased expression in TNF- α and IL-1 β) is suggested in our VDN model but may be less important or more subtle than in other articles.^{8–10,23} In VDN rats, aortic wall calcification was strongly associated with monocyte/macrophage infiltration and increased expression of TNF- α and IL-1 β ; IFN- γ mRNA, which is produced by lymphocytes and/or natural killer cells, did not change. Pio did not modify the strong association between calcium deposits and monocyte/macrophage infiltration because, when present, aortic calcified lesions were similar in nature to those observed in VDN Pio⁻; however, the frequency of calcified lesions along the aortic segment was lower in VDN Pio⁻. Moreover, the lack of correlation between IL-1 β mRNA and calcium contents in VDN Pio⁺ suggests that the antiinflammatory effect of Pio is not the only mechanism responsible for the decrease in aortic wall calcification in the VDN model.

Other hypotheses can be evoked. Pio may attenuate the recruitment of cells producing proteins involved in arterial wall calcification. Firstly, in the VDN model, arterial wall calcification is initiated by recruitment of S-100⁺ cells and deposition of extracellular S-100 calcium-binding proteins.¹² Secondly, Pio and vitamin D are ligands for nuclear receptors, which may interfere with each other,²⁴ and those modify bone calcium metabolism and at a later stage arterial wall calcification. In VDN, part of the arterial ectopic apatite deposited is of bone origin. The calcium content of the femoral bone decreases during the first 2 weeks following VDN treatment,²⁵ inhibition of osteoclasts prevents arterial calcification in vitamin D-treated rats,²⁶ and TZDs inhibit bone resorption induced by vitamin D.²⁷ Thirdly, part of the calcium deposited on the wall elastic fibers is released from smooth muscle cells following calcium overload-induced necrosis^{4,28} produced by a direct or indirect (sympathomimetic) action²⁸ of nicotine. Calcium channel blockers such as isradipine reduce aortic wall calcification in the VDN model,⁴ and TZDs block smooth muscle cell calcium channels.²⁹

Treatment with Pio halved calcium deposition, which remained, none-the-less, elevated (21-fold above non-VDN rats). In spite of this, Pio normalized EM/WS (Figure 4) in VDN rats. This suggests that the reduction of calcification is not the only way by which Pio improves wall elasticity in the VDN model and that calcification is not the only factor responsible for elastic fiber degradation. This is backed up by the observation that the regression analysis of EM/WS versus wall calcium content shows a lower slope for VDN rats

TABLE 3. Body Weight, Plasma Glucose Concentration, Heart Rate, and Percentage of Dry Weight in the Myocardium in VDN and Non-VDN Rats Treated or Not With Pio for Forty-Four Days

groups	non-VDN	VDN	ANOVA		
Body weight, g					
Pio ⁻	369±8	351±8	$P_{VDN}=0.017$	$P_{Pio}<10^{-4}$	$P_{VDN \times Pio}=0.950$
Pio ⁺	407±8†	389±5*†			
Plasma glucose concentration, mmol · L ⁻¹					
Pio ⁻	11.3±0.8	12.0±1.6	$P_{VDN}=0.989$	$P_{Pio}=0.472$	$P_{VDN \times Pio}=0.466$
Pio ⁺	11.3±1.0	12.1±0.9			
Cardiac parameters					
Heart rate, bpm					
Pio ⁻	432±11	445±13	$P_{VDN}=0.602$	$P_{Pio}=0.896$	$P_{VDN \times Pio}=0.604$
Pio ⁺	440±14	440±8			
Left ventricle (including septum), g					
Pio ⁻	0.56±0.02	0.62±0.03	$P_{VDN}=0.105$	$P_{Pio}=0.274$	$P_{VDN \times Pio}=0.132$
Pio ⁺	0.61±0.01	0.61±0.01			
Dry weight/wet weight, %					
Pio ⁻	23.4±0.4	23.1±0.3	$P_{VDN}=0.936$	$P_{Pio}=0.558$	$P_{VDN \times Pio}=0.319$
Pio ⁺	22.8±0.5	23.2±0.2			

* $P<0.05$ vs non-VDN rats, † $P<0.05$ vs Pio⁻.

treated with Pio. The normalization of EM/WS cannot be explained by a change in aortic geometry because, although Pio does reduce VDN-induced dilatation, it does not modify global wall stress. It is possible that more subtle changes in the distribution of tension throughout the wall (eg, less recruitment of stiff collagen fibers because of the less pronounced enlargement of the aorta) may account for the changes in wall integrity/component and, thus, for the normalization of the elastic properties. However, global changes in wall composition such as fibrosis (Pio has no effect on collagen content) or edema (Pio has no effect on dry weight percentage) are seemingly not involved. It is possible that Pio protects the elastic fiber network from degradation by an antiinflammatory action (decreased expression of proinflammatory cytokines), leading to a decrease in metalloprotease activity.^{8,30,31} Other potential mechanisms could include antioxidant effects and protection of endothelial function³² or some effect at the level of the angiotensin II type 1 receptor.³³ Whatever the mechanism, protection of the elastic fiber network from degradation maintained aortic wall elastic properties and structural integrity, thus preventing aortic aneurysm. It is interesting to note that dilatation is not accompanied by wall thickening in VDN.

Finally, it should be noted that the beneficial Pio effect on pulse pressure is attributable to attenuation of the fall in diastolic pressure in VDN. This would maintain coronary perfusion and may be relevant in the elderly. Pio significantly lowered pulse pressure, and it could be argued that the subsequent reduction in pulsatile wall stress could somehow attenuate the pressure-induced amplification of the physicochemical reaction of elastocalcinosis. There are arguments for and against this. Megnien et al³⁴ showed that hypertension (ie, an increase in both mean and pulse pressures) amplifies arterial calcification. However, we have shown in the VDN

model that long-term treatment with the calcium entry blocker, isradipine, lowers mesenteric artery calcification but has no effect on blood pressure (or on aortic calcification).³⁵ This has been discussed previously⁵ and the question is still unanswered as to whether increased pressure (and, thus, increased wall stress) amplifies wall elastocalcinosis.

Perspectives

In conclusion, we have shown that long-term Pio treatment protects against calcification and degradation of aortic wall elastic fibers via, at least partially, an antiinflammatory mechanism. This improves aortic wall elasticity in a rat model of elastocalcinotic arteriosclerosis, thus preventing elevation of pulse pressure and left ventricular hypertrophy. Our results may be clinically relevant in elderly patients experiencing aortic wall stiffening.

Acknowledgments

This work was funded by grants from the French Education, Research and Technology Ministry; the Regional Development Committee (Metz, France); the Greater Nancy Urban Council (Nancy, France); the Pharmacolor Association (Nancy, France); the "Fondation de la Recherche Médicale" (Lorraine Committee, France); the "Ligue contre le Cancer" (54 Committee, France); the "Fondation de France," Paris; and the "Association de la Recherche contre le Cancer" (ARC No. 5637; Paris). We thank Patrick Liminana (Pharmacology Laboratory), Aurélie Beltz (EA3446, Nancy, France), and Annie Artuso (EA3127, Montpellier, France) for help with histomorphometry, Western blot analysis, and ED-1 immunostaining.

References

- Lehmann ED, Hopkins KD, Rawesh A, Joseph RC, Kongola K, Coppack SW, Gosling RG. Relation between number of cardiovascular risk factor/events and noninvasive Doppler ultrasound assessments of aortic compliance. *Hypertension*. 1998;32:565-569.

2. Blacher J, Asmar R, Djane S, London GM, Safar ME. Aortic pulse wave velocity as a marker of cardiovascular risk in hypertensive patients. *Hypertension*. 1999;33:1111–1117.
3. Meaume S, Benetos A, Henry OF, Rudnichi A, Safar ME. Aortic pulse wave velocity predicts cardiovascular mortality in subjects >70 years of age. *Arterioscler Thromb Vasc Biol*. 2001;21:2046–2050.
4. Fleckenstein A, Frey M, Fleckenstein-Grun G. Protection by calcium antagonists against experimental arterial calcinosis. *Secondary Prevention of Coronary Heart Disease, Workshop of the International Society and Federation of Cardiology*. New York: Pyörälä K, Georg Thieme Verlag; 1983:109–122.
5. Atkinson J. Arterial calcification. Mechanisms, consequences and animal models. *Pathol Biol*. 1999;47:677–684.
6. Cantini C, Kieffer P, Corman B, Laminana P, Atkinson J, Lartaud-Idjouadiene I. Aminoguanidine and aortic wall mechanics, structure, and composition in aged rats. *Hypertension*. 2001;38:943–948.
7. Kass DA, Shapiro EP, Kawaguchi M, Capriotti AR, Scuteri A, Degroff RC, Lakatta EG. Improved arterial compliance by a novel advanced glycation end-product crosslink breaker. *Circulation*. 2001;104:1464–1470.
8. Duval C, Chinetti G, Trottein F, Fruchart JC, Staels B. The role of PPARs in atherosclerosis. *Trends Mol Med*. 2002;8:422–430.
9. Law RE, Goetze S, Xi XP, Jackson S, Kawano Y, Demer L, Fishbein MC, Meehan WP, Hsueh WA. Expression and function of PPARgamma in rat and human vascular smooth muscle cells. *Circulation*. 2000;101:1311–1318.
10. Ishibashi M, Egashira K, Hiasa K, Inoue S, Ni W, Zhao Q, Usui M, Kitamoto S, Ichiki T, Takeshita A. Antiinflammatory and antiarteriosclerotic effects of pioglitazone. *Hypertension*. 2002;40:687–693.
11. Henrion D, Chillon JM, Godeau G, Muller F, Capdeville-Atkinson C, Hoffman M, Atkinson J. The consequences of aortic calcium overload following vitamin D₃ plus nicotine treatment in young rats. *J Hypertens*. 1991;9:919–926.
12. Niederhoffer N, Bobryshev YV, Lartaud-Idjouadiene I, Giummelly P, Atkinson J. Aortic calcification produced by vitamin D₃ plus nicotine. *J Vasc Res*. 1997;34:386–398.
13. Lartaud-Idjouadiene I, Lompré AM, Kieffer P, Colas T, Atkinson J. Cardiac consequences of prolonged exposure to an isolated increase in aortic stiffness. *Hypertension*. 1999;34:63–69.
14. Niederhoffer N, Marque V, Lartaud-Idjouadiene I, Duvivier C, Peslin R, Atkinson J. Vasodilators, aortic elasticity, and ventricular end-systolic stress in nonanesthetized unrestrained rats. *Hypertension*. 1997;30:1169–1174.
15. Marque V, Kieffer P, Gayraud B, Lartaud-Idjouadiene I, Ramirez F, Atkinson J. Aortic wall mechanics and composition in a transgenic mouse model of Marfan syndrome. *Arterioscler Thromb Vasc Biol*. 2001;21:1184–1189.
16. Von Kossa J. Über die im Organismus künstlich erzeugbaren Verkalkungen. *Beitr Path Anat*. 1901;29:163–202.
17. Devaux Y, Grosjean S, Seguin C, David C, Dousset B, Zannad F, Meistelman C, De Talancé N, Mertes PM, Ungureanu-Longrois D. Retinoic acid and host-pathogen interactions: effects on the inducible nitric oxide synthase in vivo. *Am J Physiol*. 2000;279:E1045–E1053.
18. Seguin-Devaux C, Devaux Y, Latger-Cannard V, Grosjean S, Rochette-Egly C, Meistelman C, Zannad F, Mertes PM, Longrois D. Enhancement of the inducible NO synthase activation by all-trans retinoic acid is mimicked by RAR α agonist in vivo. *Am J Physiol*. 2002;283:E525–E535.
19. Ghuyssen JM, Strominger JL. Structure of the cell wall of *Staphylococcus aureus*, strain Copenhagen. I. Preparation of fragments by enzymatic hydrolysis. *Biochemistry*. 1963;5:1110–1119.
20. Neuman RE, Logan MA. The determination of collagen and elastin in tissues. *J Biol Chem*. 1950;184:549–556.
21. Mansen A, Guardioladiaz H, Rafta J, Branting C, Gustafsson JA. Expression of the peroxisome proliferator-activated receptor (PPAR) in the mouse colonic mucosa. *Biochem Biophys Res Commun*. 1996;222:844–851.
22. Huin C, Corriveau L, Bianchi A, Keller JM, Collet P, Kremarik-Bouillaud P, Domenjoud L, Becuwe P, Schohn H, Menard D, Dauca M. Differential expression of peroxisome proliferator-activated receptors (PPARs) in the developing human fetal digestive tract. *J Histochem Cytochem*. 2000;48:603–611.
23. Ricote M, Li AC, Willson TM, Kelly CJ, Glass CK. The peroxisome proliferator-activated receptor-gamma is a negative regulator of macrophage activation. *Nature*. 1998;391:79–82.
24. Hida Y, Kawada T, Kayahashi S, Ishihara T, Fushiki T. Counteraction of retinoic acid and 1,25-dihydroxyvitamin D₃ on up-regulation of adipocyte differentiation with PPARgamma ligand, an antidiabetic thiazolidinedione, in 3T3-L1 cells. *Life Sci*. 1998;62:205–211.
25. Kieffer P, Robert A, Capdeville-Atkinson C, Atkinson J, Lartaud-Idjouadiene I. Age-related calcification in rats. *Life Sci*. 2000;66:2371–2381.
26. Brice PA, June HH, Buckley JR, Williamson MK. SB 242784, a selective inhibitor of the osteoclastic V-H⁺-ATPase, inhibits arterial calcification in the rat. *Circ Res*. 2002;91:547–552.
27. Okazaki R, Toriumi M, Fukumoto S, Miyamoto M, Fujita T, Tanaka K, Takeuchi Y. Thiazolidinediones inhibit osteoclast-like cell formation and bone resorption in vitro. *Endocrinology*. 1999;140:5060–5065.
28. Hass GM, Trueheart RE, Taylor CB, Stumpe M. An experimental histologic study of hypervitaminosis D. *Am J Pathol*. 1958;34:395–431.
29. Nakamura Y, Ohya Y, Onaka U, Fujii K, Abe I, Fujishima M. Inhibitory action of insulin-sensitizing agents on calcium channels in smooth muscle cells from resistance arteries of guinea-pig. *Br J Pharmacol*. 1998;123:675–682.
30. Marx N, Schonbeck U, Lazar MA, Libby P, Plutzky J. Peroxisome proliferator-activated receptor gamma activators inhibit gene expression and migration in human vascular smooth muscle cells. *Circ Res*. 1998;83:1097–1103.
31. Li AC, Brown KK, Silvestre MJ, Willson TM, Palinski W, Glass CK. Peroxisome proliferator-activated receptor gamma ligands inhibit development of atherosclerosis in LDL receptor-deficient mice. *J Clin Invest*. 2000;106:523–531.
32. Verges B. Clinical interest of PPARs ligands. *Diabetes Metab*. 2004;30:7–12.
33. Pershadsingh HA. Peroxisome proliferator-activated receptor-gamma: therapeutic target for diseases beyond diabetes: quo vadis? *Expert Opin Investig Drugs*. 2004;13:215–228.
34. Megnien JL, Simon A, Lemarié M, Plainfosse MC, Levenson J. Hypertens promotes coronary calcium deposit in asymptomatic men. *Hypertension*. 1996;27:949–954.
35. Henrion D, Chillon JM, Capdeville-Atkinson C, Atkinson J. Effect of long-term treatment with the calcium entry blocker, isradipine, on vascular calcium overload produced by vitamin D₃ and nicotine in rats. *J Pharmacol Exp Ther*. 1992;260:1–8.